PHYSICAL REVIEW A **74**, 042722 (2006)

X-ray absorption spectra from the resonant-convergent first-order polarization propagator approach

Ulf Ekström* and Patrick Norman†
Department of Physics and Measurement Technology, Linköping University, SE-581 83 Linköping, Sweden

(Received 8 July 2006; published 27 October 2006)

The one-photon absorption cross sections of molecular systems have been determined in the high-energy region from the imaginary part of the electric dipole polarizability tensor. In contrast to commonly adopted state-specific methodologies, the complex polarization propagator approach does not require explicit consideration of the excited states and it is open-ended towards multiphoton absorption. It is shown that the electronic relaxation in the core-hole state is well accounted for in the present approach with use of standard density-functional based electronic structure methods. Sample calculations are presented of the *K*-edge x-ray absorption spectra for H_2O, CO, C_4H_4N, and C_6H_6.

DOI: 10.1103/PhysRevA.74.042722 PACS number(s): 32.80.Fb, 32.30.Rj

I. INTRODUCTION

X-ray absorption spectroscopy (XAS) is a widely used experimental technique due to its ability to characterize the local molecular structure of samples. Its sensitivity to the local molecular environment stems from the fact that, for x-rays, the photon energy is comparable to core electron ionization energies, and the hole will therefore be localized to a particular atom. The virtual orbital, on the other hand, is extended over the molecule, and, because of this, the spectroscopy probes the atomic environment. When x-ray absorption spectra are nontrivial, for example when several chemically shifted or spin-orbit splitted core orbitals are involved in the absorption process, a good theoretical model is called for in order to exhaust the information in the experiment. As of today, there exist a number of approaches for the calculation of XAS, ranging from high quality state-specific multireference configuration interaction [1] methods to more approximate ones such as the static exchange approximation (STEX) [2–4] and density-functional theory (DFT) based methods [5]. Common to all state-specific methods, however, is the fact that they are prohibitively expensive when addressing a large number of core excited states, and other issues are the treatment of dynamic correlation and electronic relaxation in multireference state approaches, the lack of systematic improvements to the STEX approach, and the limited applicability and theoretical foundation of current DFT based approaches.

Furthermore, the development of new x-ray radiation sources will enable novel x-ray spectroscopies such as femtochemistry and multiphoton absorption experiments [6,7], a development that presents new challenges for theoretical modeling. None of the approaches described above are, e.g., able to address multiphoton XAS, whereas, in the optical region, such calculations are performed for large molecular systems with polarization propagator techniques [8]. The reason for this deficiency is the electric dipole coupling between the final core excited state and all intermediate states, valence and core excited.

The main impediment in quantum chemical calculations of XAS, as compared to optical absorption, is that the final states of interest are embedded in ionization states of the more loosely bound electrons; the ionization states form a continuum that do not significantly contribute to the x-ray absorption of the core states. In standard polarization propagator approaches, such as the random-phase approximation (RPA) [9], the eigenvalues of the electronic Hessian are found by iterative techniques, and special care has to be taken to find the states of interest. In the general case, this is cumbersome, since one desires to resolve only the states contributing to the absorption, and not the large number of eigenstates in the low-energy region. Furthermore, the entire absorption edge of a particular core shell can require hundreds, or thousands, of excited states for an accurate description.

In the present work, we will demonstrate that it is possible to overcome the difficulties mentioned above by avoiding an explicit resolution of the excited states, and focusing directly on the physical observable, namely the absorption cross section. By employing a resonant-convergent first-order polarization propagator approach [10,11], where absorption is included in the formalism, it is possible to directly calculate the absorption cross section at a particular frequency without explicitly addressing the excited-state spectrum. The proposed approach is open-ended towards an extension to multiphoton absorption—in the optical as well as the x-ray region of the spectrum—and our work should be seen as a first step in this direction. Again this is possible due to the implicit treatment of *all* excited states in the calculation in the complex polarization propagator (CPP) approach. The CPP has been implemented in the Hartree-Fock, multiconfiguration self-consistent field, and Kohn-Sham DFT electronic structure theory [10,11].

Our methodology has been illustrated in a letter [12], but there are several key issues that need to be addressed in greater detail in order to provide insight to the virtues and limitations of the complex polarization propagator approach as applied to XAS. In this work, we will demonstrate how the electronic polarization in the core excited state is accounted for by the inclusion of electron correlation in the electronic structure theory, instead of, as in conventional ap-

---

*Electronic address: ulfek@ifm.liu.se
†Electronic address: panor@ifm.liu.se

proaches, by a separate optimization of the electronic density of the final state in the absorption process. In terms of the RPA equation, one way to resolve the quasistable states in the high-energy region of XAS is to limit the construction of the electronic Hessian to include only core-hole excitation channels. In the CPP approach this approximation is not introduced, and, for a given electronic structure method, we are considering the complete propagator. We will discuss the representation of continuum states with a basis set of localized atomic orbitals, and show that an identification of the ionization threshold can be made in the CPP approach by a simple scaling procedure of the basis set exponents. Water will be used as a sample system for these investigations. We will also qualify the CPP approach against experiment not only for K-edge spectra of oxygen but also for the K-edge spectra of nitrogen and carbon. We have therefore also determined the XAS spectra of carbon monoxide, benzene, and pyrrole.

II. ABSORPTION IN MOLECULAR MATERIALS

With magnetic interactions neglected, the energy loss of an electromagnetic field in a linearly absorbing media is related to the dielectric function through the Poynting theorem [13]

$$\left\langle \frac{d}{dt}\frac{\text{absorbed energy}}{\text{volume}} \right\rangle_T = 2\omega \,\text{Im}\, \epsilon(\omega)\langle \mathbf{E}(\mathbf{r},t)\cdot\mathbf{E}(\mathbf{r},t)\rangle_T, \tag{1}$$

where the angular brackets indicate the average over one period of oscillation T. For dilute substances, the macroscopic dielectric constant is related to the microscopic molecular polarizability $\alpha(\omega)$ through the Clausius-Mossotti equation

$$\alpha = \frac{3}{N}\left(\frac{\epsilon/\epsilon_0 - 1}{\epsilon/\epsilon_0 + 2}\right) \approx \frac{1}{N}(\epsilon/\epsilon_0 - 1), \tag{2}$$

where N is the number density of the substance. The absorption cross section is directly related to the energy loss and density of the medium, and, correspondingly, it is equal to

$$\sigma(\omega) = \frac{4\pi\omega}{c}\,\text{Im}\,\alpha(\omega). \tag{3}$$

By introducing damping terms γ_n that correspond to the inverse lifetimes of the exponentially decaying excited states of the system, the molecular polarizability can be written as a sum-over-states expression

$$\alpha_{\alpha\beta}(\omega) = \hbar^{-1}\sum_{n>0}\left\{\frac{\langle 0|\hat{\mu}_\alpha|n\rangle\langle n|\hat{\mu}_\beta|0\rangle}{\omega_{0n} - \omega - i\gamma_n} + \frac{\langle 0|\hat{\mu}_\beta|n\rangle\langle n|\hat{\mu}_\alpha|0\rangle}{\omega_{0n} + \omega + i\gamma_n}\right\}, \tag{4}$$

where $\hat{\mu}_\alpha$ is the electric dipole operator along the molecular axis α and ω_{0n} is the transition frequency between the ground state $|0\rangle$ and the excited state $|n\rangle$. In practice, the inverse lifetimes of the excited states is set to a common value in the calculation, i.e., $\gamma_n = \gamma$, although there are no restrictions as such built into the CPP approach.

If we instead consider the polarizability as a function of a complex frequency argument z, i.e., z takes the place of the real frequency ω in Eq. (4), then an integration along a contour C that encloses the poles of the right half plane gives the result

$$\text{Im}\int_C z\alpha_{\alpha\beta}(z)dz = 2\pi\sum_n \omega_{0n}\langle 0|\hat{\mu}_\alpha|n\rangle\langle n|\hat{\mu}_\beta|0\rangle, \tag{5}$$

independent of the values of the inverse lifetimes γ_n. In the limit of small γ_n, the integrand can be related to the linear absorption cross section in Eq. (3) and we get

$$\begin{aligned}\frac{m_e}{3\pi e^2}\,\text{Im}\int_C z\alpha(z)dz &= \frac{4m_e}{3ce^2}\int_0^\infty \sigma(\omega)d\omega \\ &= \sum_n \frac{2m_e\omega_{0n}}{3\hbar e^2}|\langle n|\hat{\mu}|0\rangle|^2 = \sum_n f_{n0} = N_e,\end{aligned} \tag{6}$$

where m_e is the electron mass, e is the elementary charge, and N_e is the number of electrons, and, in the last step, we used the Thomas-Reiche-Kuhn sum rule for the oscillator strengths f_{0n}. We have thus seen that, in the limit of small inverse lifetimes, there is an equivalence of whether one determines the linear absorption spectrum from the imaginary part of the electric dipole polarizability or from the oscillator strengths. The former way is adopted in this work and avoids the explicit resolution of the excited states whereas the latter way involves the determination of the eigenvectors of the electronic Hessian.

In the random-phase approximation and with a common lifetime broadening for all excited states, the polarizability is given by the solution to the response equation [10,11]

$$\alpha_{\alpha\beta}(\omega) = -\mu_\alpha^{[1]\dagger}[E^{[2]} - (\omega + i\gamma)S^{[2]}]^{-1}\mu_\beta^{[1]}, \tag{7}$$

where $\mu_\alpha^{[1]}$ is the electric-dipole property gradients along the molecular axis α, $E^{[2]}$ is the electronic Hessian, and $S^{[2]}$ is a metric (overlap matrix). In a resonant-divergent propagator approach (γ=0), Eq. (7) cannot be used to calculate the absorption, and one instead solves the generalized eigenvalue equation

$$\det[E^{[2]} - \omega S^{[2]}] = \det\left[\begin{pmatrix} A & B \\ B^* & A^* \end{pmatrix} - \omega\begin{pmatrix} 1 & 0 \\ 0 & -1 \end{pmatrix}\right] = 0, \tag{8}$$

directly for the excitation energies and transition moments. In this sense it does not matter if one uses Eq. (8) or the linear-response function of Eq. (4) to construct the absorption spectrum, as we have discussed above. In practice it is, however, not feasible to construct the electronic Hessian $E^{[2]}$, and Eq. (8) must be solved iteratively for a small number of roots. The problems with this approach for x-ray absorption are outlined in the Introduction, and we may contrast this with an approach based on Eq. (3). Here the absorption at a particular frequency can be computed, at a constant computational cost and memory usage regardless of how many states are involved. In this way the energy region of interest can be sampled with an energy spacing corresponding to the linewidths γ_n. In practice we consider a constant $\gamma_n = \gamma$ as a fitting parameter depending on the experimental resolution in the energy range of interest. The cost of the calculation is thus determined from the resolution of the experiment. In the case of standard RPA, the character of the excited state and an interpretation in terms of orbitals can be obtained from the solution vectors to Eq. (8), whereas, in the present approach, the same information is retained from the imaginary part of the frequency-dependent response vector $N^B(\omega) = [E^{[2]} - (\omega + i\gamma)S^{[2]}]^{-1}\mu_\beta^{[1]}$ in Eq. (7).

An extension to two-photon absorption would involve the imaginary part of the second-order hyperpolarizability, $\gamma(-\omega;\omega,-\omega,\omega)$, as obtained from a cubic response function. The procedure would otherwise follow the outline given here for linear absorption.

III. RESULTS AND DISCUSSION

A. Computational details

To show the features of the CPP approach we have calculated the *K*-edge spectra of oxygen in water, carbon in benzene and carbon monoxide, and nitrogen in pyrrole. The calculations are based on Eq. (7) and refer to the Hartree-Fock (HF) and Kohn-Sham DFT electronic structure methods. The x-ray absorption spectra have been calculated using an implementation [10] in the DALTON program [14], and, for reasons of comparison, we have also employed the STEX method with use of the same program. The calculations have been performed using the triply augmented correlation consistent double-ζ basis set of Dunning (t-aug-cc-pVDZ) [15]. Because of our use of finite Gaussian-type orbitals (GTOs) in the basis set, we cannot treat the region above the ionization edge and results are restricted to photon energies below the core ionization threshold.

B. Experimental spectra

Four molecules have been chosen to illustrate the effectiveness of the CPP method, one diatomic molecule (CO), one triatomic (H_2O), and two aromatic systems, C_6H_6 and C_4H_4N. The experimental near-edge x-ray absorption fine-structure (NEXAFS) spectra of these molecules are available in the literature and have been discussed in previous publications [16,17]. For completeness we make a short review of the main characteristics of these spectra.

The valence part of the H_2O spectrum (Fig. 1) is made up of peaks corresponding to excitations from the oxygen $1s$ to the virtual $4a_1$, $2b_1$, and $2b_2$ orbitals. The intensity of each absorption peak is dependent on the local *p* character of the empty orbitals at the oxygen nucleus, which gives stronger intensities for excitations to the B_1 and B_2 states that involves orbitals with nodes on the oxygen atom. Vibrational states are not individually resolved in the experimental spectrum, and, to good approximation, the line shapes are symmetric. By integrating the absorption cross section we obtain experimental intensity ratios of 1:1.3:0.7 for the three lowest peaks.

In carbon monoxide, as well as in the aromatic molecules, the dominant spectral feature is the strong $1s \rightarrow \pi^*$ transition.

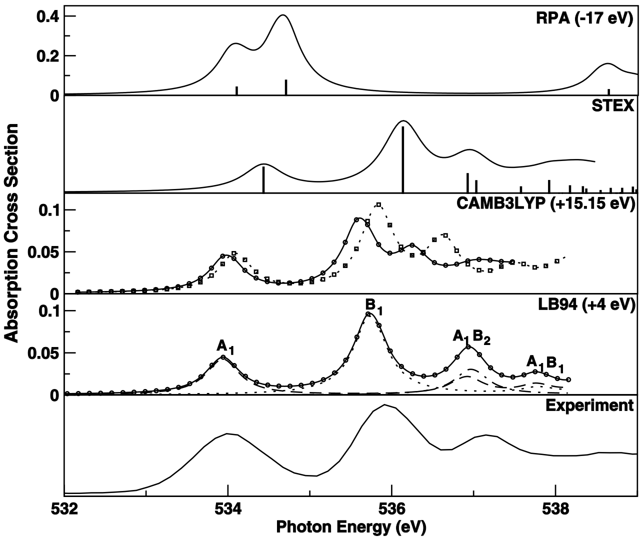

FIG. 1. *K*-edge NEXAFS spectrum of water. The absorption cross sections from CPP calculations are reported in atomic units. For the RPA results, bars show RPA excitation energies and oscillator strengths in arbitrary units, while the solid curve shows the results from a CPP-HF calculation. All DFT results are obtained with the CPP method: the CAM-B3LYP results are obtained with 65% (circles) and 100% (dashed line) long-range Coulomb interaction; the LB94 results show individual components and averaged value (full line). The spectra have been shifted by the amounts indicated in the figure. The experimental results are taken from Ref. [16].

Like in the case of water, the vibrational structures, or asymmetrical line shapes, are not resolved in the experiment. In benzene there are six identical carbon atoms, possibly giving rise to interference effects between the excitation channels. However, this effect has been considered negligible in previous theoretical studies [18].

C. Electron correlation and electronic relaxation

It is well known that the large electronic relaxation effects in core excited states prohibits a successful use of the time-dependent Hartree-Fock approximation (or RPA, as commonly denoted in the literature) [2,4]. This failure is illustrated by the RPA and CPP-HF calculations on water that are presented in Fig. 1.

The RPA excitation energies and oscillator strengths have been computed by restricting the excitation channels to only those leaving a hole in the oxygen $1s$ orbital. These calculations give too high excitation energies, and the spectrum is “stretched” in energy, giving much too large energy separations between the absorption peaks and the ionization threshold. In addition to these effects the general shape of the spectrum is not in agreement with the experiment. On the other hand, the agreement between RPA and CPP-HF is in this case very good, indicating that the deficiency of the RPA calculation does not lie in the exclusion of channel interaction in this case. The failure of these calculations to provide a spectrum in reasonable agreement with experiment lies instead in the lack of electron correlation in the underlying electronic structure method.

Presented from this perspective, electronic relaxation is an effect of electron correlation. The CPP approach, however, is straightforward to combine with any electronic structure method and it thus has the potential of providing the exact electronic spectrum in the valence as well as core regions of the spectrum. We expect the electronic relaxation in the core-hole state to be an effect mainly due to dynamic correlation and we focus therefore at electronic structure methods designed to retrieve dynamic rather than static correlation. Coupled cluster approaches would be suitable in this respect but the CPP method has yet to be implemented in this case and an evaluation of this combination can, at present, therefore not be made. Instead, in this work we adopt the Kohn-Sham DFT approach with use of some of the standard adiabatic exchange-correlation functionals that have been presented in the literature over the past one and a half decades.

The principal prospects of DFT based approaches are apparent to everyone, but unfortunately there are, and probably always will be, several issues that one must consider in practical use. For instance, the standard DFT functionals suffer from self-interaction problems that lead to severely underestimated core-excitation energies. This problem has also been noted for valence charge-transfer states [19,20], where the cause of the problem is essentially the same. Due to self-interaction the Coulomb interaction between the hole and the excited electron is not treated correctly whenever there is little spatial overlap between the two, as typically occurs for high-energy absorption such as XAS. For this reason, we have employed two different density functionals designed for correct description of Coulomb interactions, namely the LB94 [21] and CAM-B3LYP [22] functionals. For CAM-B3LYP we present results both for a full asymptotic Coulomb interaction as well as for a scaled interaction including only 65%. The latter scaled functional is suggested in Ref. [22] as parametrized for valence charge-transfer excitations, but we find that 100% asymptotic Coulomb interaction improved the mixed valence-Rydberg part of the water spectrum as seen in Fig. 1. Both LB94 and CAM-B3LYP(100%) show a slight "compression" of the absorption below the ionization threshold, and for CAM-B3LYP(65%) the compression is even greater due to the inexact asymptotic behavior of this functional. We note that a small compression is present also in the STEX spectrum, in this case due to overscreening in the ionic reference state. The calculated intensity ratios for the three lowest peaks are 1:1.9:0.7 in the case of CAM-B3LYP(100%), and 1:1.6:1.05 for LB94. Considering the two lowest peaks, the results obtained with the LB94 functional agree well with the experiment intensity ratios of 1:1.3. For the third peak it is difficult to make a quantitative comparison since it is not as well isolated in the experiment. In general the energy splittings of absorption peaks are well reproduced in the theoretical calculations.

Regarding the aspects of electron correlation and electronic relaxation in the core-hole state, we conclude that CPP-DFT is indeed a viable approach as long as a correct description of the Coulomb interactions is provided in the functional; the quality of the CPP-DFT spectra are rivaling or exceeding those of STEX calculations. However, the absolute energies in the theoretical XAS spectra are underestimated to a varying degree due to self-interaction, and, in a separate publication, we will discuss how these errors can be strongly reduced for the standard functionals used here. We stress, however, that the effect of the observed errors inflicts a constant shift of the absorption energies, and it does not hamper the applicability of the CPP method for XAS.

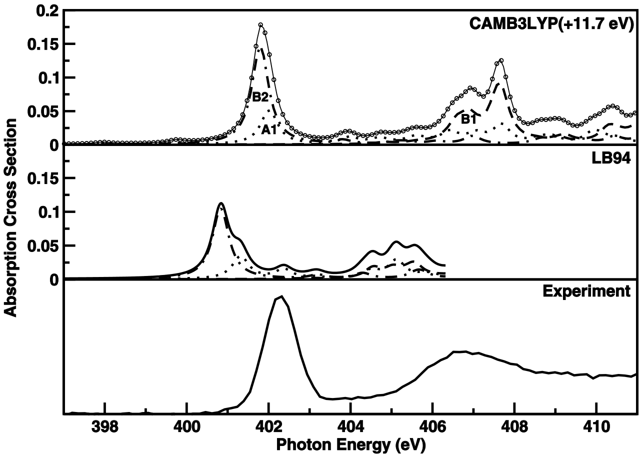

FIG. 2. Nitrogen K-edge NEXAFS spectrum of pyrrole. The absorption cross sections from CPP calculations are reported in atomic units. Symmetry components of the absorption shown by dotted (A_1), dashed (B_1), and dot-dashed (B_2) lines. The experimental results are taken from Ref. [17].

D. Polarization dependence in the x-ray absorption

An important aspect in the analysis of x-ray absorption spectra is the comparison of spectra obtained with different polarizations of the incident light; it provides information on the molecular orientation on surfaces and it allows for a characterization of the excited states.

At first, due to the implicit treatment of the excited states in the CPP approach, it may appear as if one loses the possibility to characterize the core excited states. But to the same degree as in the experiment, this information is contained in the light polarization dependence of the absorption. In Fig. 1, in the LB94 spectrum, we plot the results corresponding to the imaginary part of the individual components of the polarizability $[\alpha_{\alpha\alpha}(\omega)]$. The state lowest in energy acquires its intensity from absorption of light polarized along the molecular principal axis and thus corresponds to an $^1A_1$ state. The second peak in the spectrum is a $^1B_1$ state whereas higher-lying peaks are of mixed symmetries. We thus conclude that the polarization dependence of the absorption is given by considering the individual tensor component of the polarizability, and that this can be used as a basis for a symmetry analysis of the participating states.

In the case of the nitrogen K-edge spectrum of pyrrole presented in Fig. 2, the polarization analysis reveals that the peak at 402 eV is the sum of the contributions from states of two different symmetries, namely, $^1B_2$ and $^1A_1$. The LB94 functional gives a larger splitting of the B_2 and A_1 components of this peak as compared to both the CAM-B3LYP functional and also the experiment. Contrary to the carbon

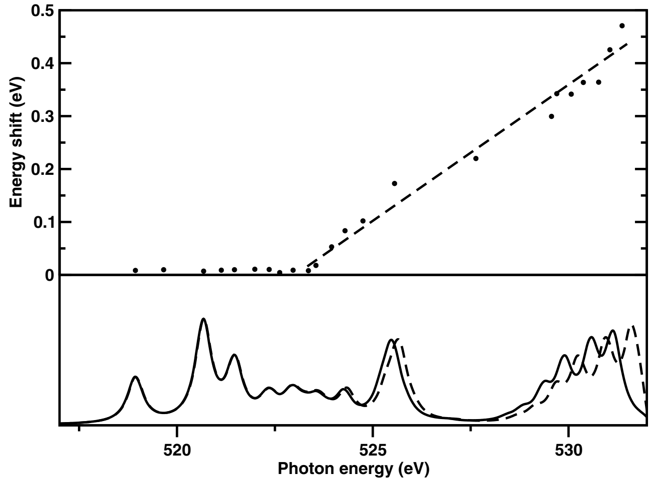

FIG. 3. The effect of basis set scaling on the absorption above and below the 1*s* ionization energy of water. The circles (above) show the energy shift of each maximum and minimum of the absorption. The two absorption curves (below) have been computed with the basis set exponents scaled by 0.9801 (whole line) and 1.0201 (dashed line), respectively.

and oxygen *K*-edge spectra under consideration, the CAM-B3LYP(100%) nitrogen spectrum is stretched compared to the experiment, instead of compressed.

E. Estimating the quality of the basis set

The calculations in this work have been performed in a GTO basis set, and these basis functions do not allow for a proper description of the continuum states. Care therefore has to be taken to ensure that the character of the resolved states is such that it is well described with the chosen basis functions. But since we do not resolve the individual Rydberg states, converging on the ionization energy of the system, there is no clear way to determine in what energy range the calculated absorption is a good approximation to the true absorption. It is clear, however, that the excited states above the ionization threshold as approximated in a finite GTO basis will not satisfy the virial theorem. This is because continuum orbitals cannot be accurately represented in such a basis. We therefore propose a stability criterion based on the change in the absorption spectrum with respect to a uniform scaling of the basis set. In Fig. 3 we show the effect of scaling the basis set exponents, on the positions of the absorption maxima and minima in the water absorption spectrum. As can be seen in the figure, the energy shifts are small and approximately constant below the ionization threshold, while above the threshold the shifts are increasing linearly with photon energy. In this way we are able not only to determine the ionization threshold but also the valid energy range for a particular basis set.

In some cases it may occur that spurious absorption peaks appear as an artifact of a given basis set. Such peaks correspond to valence-continuum excitations, and are undesired artifacts of the finite basis. However, augmenting the basis with diffuse functions may not always cure the problem, only shift these spurious peaks, and we therefore propose to restrict the excitation space only to include virtual orbitals with eigenvalues below a given threshold (high enough not to influence the core-valence excitations). The CO molecule can be used to illustrate these effects of the finite basis set, see Fig. 4. For this purpose the aug-cc-pVDZ basis has been augmented with a diffuse set of $[7s7p7d]$ functions, and compared to an augmentation using $[22s22p22d]$ functions. For calculations with the CAM-B3LYP functional the effect of the change in basis sets is negligible, showing that the $[7s7p7d]$ augmentation is already sufficient in the energy region of interest. However, with the LB94 functional and the smaller basis a spurious peak appears just below 292 eV in Fig. 4. This peak corresponds to an excitation from the valence to a virtual orbital with an energy close to 300 eV. We also note that intensity is transferred from the real absorption peak to the spurious peak. In the calculation with the larger basis set this peak is absent, showing that it is indeed an unphysical absorption peak.

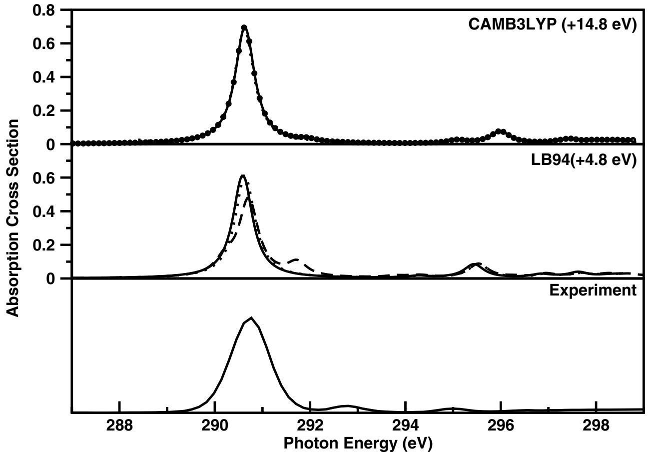

FIG. 4. Carbon *K*-edge NEXAFS spectrum of CO. The absorption cross sections from CPP calculations are reported in atomic units. Results are obtained with the aug-cc-pVTZ basis sets with additional augmentations of $[22s22p22d]$ (full line) and $[7s7p7d]$ (dotted and dashed lines). Dashed line shows artifacts of the finite basis set. The experimental results are taken from Ref. [16].

In the general case it is not practical to identify spurious peaks by determining the responses to changes in the basis set as indicated for carbon monoxide in Fig. 4. Instead we have implemented an energy cutoff in the excitation space, based on the eigenvalues of the virtual orbitals. In Fig. 4 (dotted line) we present the absorption calculated with the $[7s7p7d]$ augmented basis set and with inclusion only of virtual orbitals with eigenvalues less than 150 eV. As can be seen in the figure, this spectrum is virtually identical to that obtained with the $[22s22p22d]$ augmented basis set. We therefore recommend that an energy cutoff in the excitation space is always employed, unless stability with respect to the basis can be assured in some other way.

F. Chemically identical and nonidentical atoms

In the case of benzene there are six chemically identical carbon atoms and it seems natural to require that the elec-

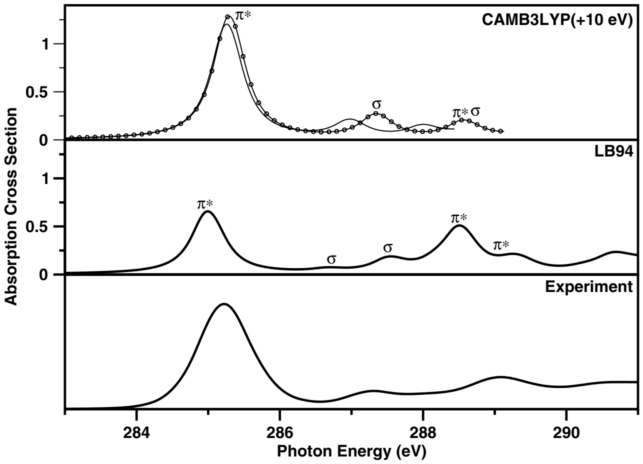

FIG. 5. *K*-edge NEXAFS spectrum of benzene. The absorption cross sections from CPP calculations are reported in atomic units. The CAM-B3LYP results are computed using 65% and 100% (circles) long-range Coulomb interaction. The experimental results are taken from Ref. [16].

tronic ground as well as excited states reflects this symmetry. In the CPP approach there is no difference in the treatment of valence and core excitations and all electronic states will therefore span the irreducible representations of the molecular point group. In state-specific approaches, such as, e.g., the STEX method, there is a choice as to whether or not one localizes the core hole to a specific atomic center [23]. A localization of the core hole and thereby a symmetry broken wave function in the excited state may be a consequence of the vibrational Jahn-Teller coupling. Our calculations for the carbon *K*-edge spectrum of benzene in Fig. 5 account for excitations from all six core regions, but the effect Jahn-Teller localization has on the electronic spectrum is assumed to be small. This is, however, not the same as saying that the vibrational effects as such are small, but a discussion of vibrational profiles is beyond the scope of the present work. The calculated benzene spectra show the same compression as seen in the water spectra; the best agreement with experiment is obtained with the LB94 functional. The absolute energy predicted by CPP-LB94 is also in good agreement with the experiment, in contrast to the case of the oxygen *K*-edge spectrum of water. It is also seen that, compared with the CAM-B3LYP functional, results obtained with the LB94 functional provide better relative energies for the higher π^* states, although the intensity of the second π^* peak is overestimated. Considering the consistently improved quality of results obtained with the CAM-B3LYP(100%) functional as compared to the CAM-B3LYP(65%) functional, we recommend use of the former in future calculations of XAS.

In large molecules of low symmetry, there may be a large number of chemically nonequivalent atoms of the same type. In such a situation the excited state should of course be represented by a core-hole localized wave function regardless of a discussion of vibration, and it is desired from theory to be able to assign spectral peaks to atomic sites. In state-specific approaches one would go about this task by calculating the individual spectra with core holes localized to the different atomic sites, one at a time. The final spectrum would be obtained by adding the atom specific spectra. We wish to emphasize that, in the CPP approach, the complete spectrum is obtained in one single calculation which may be highly beneficial for large systems. Despite this, there is no loss of information in the CPP method as compared to state specific methods. The assignment of peaks to atomic sites is readily done after an orbital analysis is done of the response vectors in Eq. (7) that correspond to the frequencies of the peaks.

IV. SUMMARY AND CONCLUSIONS

Successful assignment of spectral peaks in the experiment, based on theoretical calculations, relies on accurate predictions of both intensities and excitation energies. The sample calculations presented in this work show that the *complex polarization propagator* (CPP) approach is capable of providing high quality results in both these aspects.

We have presented a computational approach for the calculation of high-energy photoabsorption in molecular materials; as a matter of fact, the proposed methodology is in form and implementation identical regardless of the energy region of interest so valence, ultraviolet, and x-ray regions of the spectrum are included in one common treatment. The calculation of absorption is based on the imaginary part of the electric dipole polarizability which we determine with a resonant-convergent CPP approach. The theory is applicable to all standard electronic structure theories, and it is therefore open-ended towards inclusion of electron correlation in a way that, for instance, the static exchange approximation (STEX) is not. The *exact* results for the electronic absorption in the x-ray region is therefore available under the same conditions as those found for valence transitions. Since the CPP method rests solely on the optimization of the electronic ground state, it avoids all problematic issues involved with the optimization of the highly excited final state in the absorption process as well as it preserves orthogonality between the initial and final states.

Admittedly, for the CPP method to provide highly accurate x-ray absorption spectra there are strong demands on the description of electron correlation in the electronic structure method at hand. The reason for this is that, in the CPP approach, the charge polarization of the core hole in the final state is described as an effect of electron correlation whereas, in separate-state based methods, it is included by the optimization of the excited state. So, while the Hartree-Fock approximation in many cases provides accurate results for core excitations in the STEX approach it may not be all that useful in the CPP approach. However, at the same time as electron correlation may be the stumbling block of the CPP method it is also one of its strong points by being the sole factor to determine the quality of the calculation. During the last decade it has become clear that density-functional theory (DFT) places itself as one of the most important tools in quantum chemistry. As far as the time-dependent Kohn-Sham DFT method is concerned, its most appealing feature, apart from being cost effective, is that it is an exact theory if only the true nonadiabatic exchange correlation functional was known. We therefore argue that the CPP approach to the calculation of absorption will yield a powerful combination with DFT, and this approach will benefit from the development of more accurate functionals in chemistry which is a very active research area of general interest and importance. In fact, CPP-DFT calculations do provide yet another sensitive probe in the development of exchange correlation functionals.

Not only do CPP-DFT calculations have a potential of being highly accurate, they will also be applicable to very large systems with the development of linear scaling techniques in DFT. We emphasize that there are no specific issues involved with the complex polarization propagator technique; in the case of DFT, it is formulated and based on the same Fock matrix routines as other modules of the program and it will therefore benefit directly from improvements in the handling of two-electron integrals. The calculation of x-ray absorption spectra for large-scale systems also reveals another strong feature of the CPP approach, namely that the absorption from all atomic centra is included. In traditional methods that involve the optimization of the final state one would localize the hole orbital to a specific atomic center and repeat the calculation for all symmetry independent centra. Such a procedure is of course prohibitive for calculations on large systems with low spatial symmetries.

The CPP approach as presented here neglects vibrational effects in the absorption spectra. In many cases there is no need to consider this effect, while in some other cases it may be absolutely essential for a correct interpretation. This issue is, however, not specific to the proposed CPP method and further discussion of vibrational profiles is beyond the scope of the present work.

We point out that an extension of the present approach from one-photon to multiphoton absorption is provided by turning to the imaginary part of the second, fourth, etc., hyperpolarizability. In the case of multiphoton x-ray absorption, the CPP approach would be the only available formulation as of today, and the reason is the coupling of the initial and final states in the absorption process to *all* intermediate states in the system. This coupling would be automatically included with the CPP technique since the whole excitation and de-excitation manifolds are considered in the construction of the propagator, and, for the same reason, the CPP method is also gauge invariant.

The CPP approach is not only possible to combine with any electronic structure method, thereby choosing the description of the *N*-particle space, but it can also be combined with different descriptions of the one-particle space. In other words, the present implementation is based on the use of Gaussian-type orbitals but could well be modified to include other types of basis functions. The main reason for such a development in the context of x-ray absorption spectroscopy would be the possibility to address the states in the continuum above the core ionization edge.

ACKNOWLEDGMENT

The authors acknowledge computing time from the National Supercomputer Centre (NSC), Sweden.

---

[1] G. Fronzoni, M. Stener, and P. Decleva, Chem. Phys. **246**, 127 (1999).
[2] H. Ågren, V. Carravetta, O. Vahtras, and L. Petterson, Theor. Chim. Acta **97**, 14 (1997).
[3] U. Ekström, P. Norman, and V. Carravetta, Phys. Rev. A **73**, 022501 (2006).
[4] H. Ågren, V. Carravetta, O. Vahtras, and L. Petterson, Chem. Phys. Lett. **222**, 75 (1994).
[5] L. Triguero and L. Petterson, Surf. Sci. **398**, 70 (1998).
[6] T. Sekikawa, A. Kosuge, T. Kanai, and S. Watanabe, Nature (London) **432**, 605 (2004).
[7] D. Norman, J. Synchrotron Radiat. **8**, 72 (2001).
[8] P. Macak, P. Cronstrand, A. Baev, P. Norman, F. Gel'mukhanov, Y. Luo, and H. Ågren, in *Nonlinear Optical Responses of Molecules, Solids and Liquids: Methods and Applications*, edited by M. G. Papadopoulos (Research Signpost, Kerala, India, 2003).
[9] J. Olsen and P. Jørgensen, J. Chem. Phys. **87**, 3235 (1985).
[10] P. Norman, D. M. Bishop, H. J. Aa. Jensen, and J. Oddershede, J. Chem. Phys. **115**, 10323 (2001).
[11] P. Norman, D. M. Bishop, H. J. Aa. Jensen, and J. Oddershede, J. Chem. Phys. **123**, 194103 (2005).
[12] U. Ekström, P. Norman, V. Carravetta, and H. Ågren, Phys. Rev. Lett. **97**, 143001 (2006).
[13] J. D. Jackson, *Classical Electrodynamics*, 3rd ed. (Wiley, New York, 1999).
[14] DALTON, a molecular electronic structure program, Release 2.0 (2005), see http://www.kjemi.uio.no/software/dalton/dalton.html
[15] T. H. Kendall, R. A. Dunning, Jr., and R. J. Harrison, J. Chem. Phys. **96**, 6769 (1992).
[16] A. Hitchcock, J. Electron Spectrosc. Relat. Phenom. **25**, 245 (1982).
[17] D. C. Newbury, I. Ishii, and A. P. Hitchcock, Can. J. Chem. **64**, 1145 (1986).
[18] H. Ågren and V. Carravetta, Chem. Phys. **196**, 47 (1995).
[19] A. Dreuw and M. Head-Gordon, J. Am. Chem. Soc. **126**, 4007 (2004).
[20] R. Bartlett, V. Lotrich, and I. Schweigert, J. Chem. Phys. **123**, 062205 (2005).
[21] R. van Leeuwen and E. J. Baerends, Phys. Rev. A **49**, 2421 (1994).
[22] T. Yanai, D. P. Tw, and N. C. Handy, Chem. Phys. Lett. **393**, 51 (2004).
[23] H. Ågren, P. S. Bagus, and B. O. Roos, Chem. Phys. Lett. **82**, 505 (1981).